Asian Journal of Chemistry; Vol. 37, No. 6 (2025), 1271-1281

ASIAN JOURNAL OF CHEMISTRY

https://doi.org/10.14233/ajchem.2025.33699

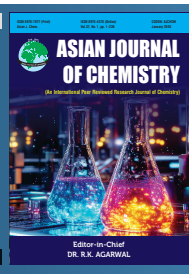

Exploring the DNA Interaction and Antimicrobial Screening of Mixed Ligand Transition Metal(II) Complexes containing Isoniazid-Lawsone Schiff Base: Synthesis, Structural Elucidation and Molecular Docking

L. RAMGEETHA and K. ARUNSUNAI KUMAR*

Research Department of Chemistry, V.H.N.S.N. College (Autonomous), (Affiliated to Madurai Kamaraj University, Madurai), Virudhunagar-626001, India

*Corresponding author: E-mail: arunsunaikumar@vhnsnc.edu.in

Received: 8 March 2025; *Accepted*: 17 April 2025; *Published online*: 27 May 2025; AJC-21997

Designing of novel metal-based molecular drugs is an effective approach to fight against the ongoing threat of antimicrobial, anticancer and antioxidant resistance. With this objective, in current work, novel mixed ligand Cu(II), Co(II), Ni(II) and Zn(II) complexes have been designed and prepared by coordinating isoniazid Schiff base as main ligand and lawsone as co-ligand. Moreover, the synthesis of these complexes have been explored with the purpose of creating stable and planar co-ligand (lawsone), thereby investigating their DNA interaction ability and other biological applications. The geometrical characteristics of these synthesized complexes were examined by elemental analysis, UV-Vis, FT-IR, NMR, Mass and EPR spectral analyses and conductivity measurements. The observed spectral data support an octahedral geometry of the complexes. The low molar conductance value specifies the non-electrolytic nature of the synthesized complexes. Their magnetic susceptibility and EPR spectral data confirm the monomeric nature of all the metal(II) complexes. The interaction between the complexes and *ct*-DNA is evaluated using electronic absorption titration and viscosity measurements, cyclic voltammetry and molecular modelling studies. DNA study reveals that the complexes have intercalation type of binding. The MIC values of the synthesized complexes expose their better antimicrobial inhibiting features than the ligand. DFT studies were also carried out using Gaussian 09 software 6-31G/B3LYP set. Moreover, the molecular docking interaction was done in order to support the *in vitro* DNA interaction experiments. The conclusions of all the studies reveal that Cu(II) complex exhibits good biological characteristics than the free ligand and other metal(II) complexes.

Keywords: Lawsone complexes, Isoniazid Schiff base complexes, DNA binding, Antimicrobial study, Molecular docking.

INTRODUCTION

Metal complexes involving Schiff bases are considered privileged ligands, as they can be readily synthesized through the condensation of carbonyl compounds (aldehydes or ketones) with primary amines. The azomethine nitrogen, which is sp^2 hybridized and contains a lone pair of electrons, exhibits excellent chelating properties–particularly when donor atoms such as oxygen or sulphur are positioned near the nitrogen [1,2]. Schiff bases readily form complexes with transition metal ions, making them a significant research focus since the 19th century. Their complexes have acquired substantial consideration due to their stability, chelating ability and biological applications, particularly in medicinal and pharmaceutical sciences [3]. Chelation with metal ions enhances the biological activity of Schiff bases, with N, S and O donor ligands playing a crucial role in tumour inhibition and antimicrobial activity. Transition metal complexes interact strongly with DNA through covalent and non-covalent mechanisms, which is essential for their antifungal, anticancer and antibacterial effects [4-6]. Notably, first-row transition metal complexes such as Cu(II), Ni(II), Co(II) and Zn(II) exhibit remarkable pharmacological potential [7,8].

Schiff bases exhibit a broad range of applications including antimicrobial, anticancer, antioxidant and antiviral properties [9-12]. Specifically, Schiff bases resulting from aromatic aldehydes with an *ortho*-hydroxyl group are particularly valuable, as they act as bidentate ligands for metal coordination. Salicylaldehyde-derived Schiff bases are well-documented for their antimicrobial, antioxidant, cytotoxic and anti-Alzheimer properties [13]. In this study, lawsone (2-hydroxy-1,4-naphtho-

quinone) is introduced as a co-ligand instead of chrysin to further investigate its biological effects [14]. Lawsone, a major bioactive naphthoquinone found in the henna plant (*Lawsonia inermis*), has been used in traditional medicine for treating [15] leprosy, smallpox, chickenpox and even HIV [16]. It is also known for its free radical scavenging [17] and antitumor properties [18].

It is known that several transition metal complexes exhibit redox activity, they have been extensively studied as DNA cleavage agents and potential DNA-targeted anticancer drugs [19]. The binding of small organic and inorganic molecules to DNA can interfere with essential processes such as transcription and replication, providing a strategic approach to combat diseases like cancer [20-22]. The three-dimensional structure of DNA facilitates drug targeting, making it easier to identify binding sites, detect conformational changes and predict drug interactions [23,24]. Metal complexes incorporating *d*-block elements have been widely explored for their nuclease-like activity, where their redox properties generate reactive oxygen species that induce DNA cleavage *via* strand scission or base modification [25]. Isoniazid (isonicotinylhydrazide), a well-known antimicrobial agent, has also demonstrated promising biological activity. However, its side effects can be minimized by Schiff base formation, likely due to the deactivation of the amino group [26]. Moroever, the mixed-ligand complexes offer a synthetic strategy to fine-tune the properties of metal complexes, leading to enhanced biological activity. Considering these insights, this work focuses on the fabrication and structural validation of Cu(II), Co(II), Ni(II) and Zn(II) mixed-ligand complexes, incorporating isoniazid and lawsone as bio-ligands. The synthesized complexes were characterized using spectral studies like UV-Vis, IR, NMR, mass spectrometry and analytical studies like molar conductivity, magnetic susceptibility, elemental analysis. Their DNA binding and antibacterial properties were evaluated to explore their therapeutic potential [27,28].

The primary goal of designing antimicrobial compounds is to inhibit pathogenic microbes without causing harmful side effects. In this context, the synthesized metal(II) complexes were screened against various bacterial and fungal strains. Moreover, density functional theory (DFT) calculations and docking simulations were conducted to compare experimental and *in silico* results, offering deeper insights into the binding interactions. These computational methods provide valuable predictions about the binding modes of Schiff base ligands and their metal complexes with DNA, further supporting their potential as anticancer agents [29,30].

EXPERIMENTAL

All chemicals utilized were of analytical grade acquired from Sigma-Aldrich, while the metal(II) salts were bought from Merck Ltd., India. Before being used, the organic solvents were extracted from the proper drying agents.

Characterization: A Perkin-Elmer 240C elemental analyzer was employed to conduct carbon, hydrogen and nitrogen elemental analyses. Infrared studies were done on Shimadzu FT-IR spectrophotometer by means of KBr technique in the 4000-400 cm^{-1} range. Utilizing TMS as an internal reference, the NMR spectra were measured using a Bruker DPX 300 spectrometer. The JASCO V-530 UV-Vis spectrophotometer was utilized to investigate the absorption spectra. Cyclic voltammetric investigations were performed employing CHI 620C electrochemical analyser. Measurements were made using acetonitrile as the solvent containing 0.2 M TMEDA at 300 K with 10^{-3} M metal complex *via* nitrogen purging. Glassy carbon was chosen as the working electrode, platinum wire was employed as the auxiliary electrode and Ag/AgCl functioned as the reference electrode for the CV measurements. Glassy carbon electrode, a platinum wire electrode and Ag/AgCl electrode were utilized as the working, counter and reference electrodes respectively. The electrospray ionization run on a MICROMASS Q-TOF mass spectrometer was employed for mass spectral studies. The well diffusion method was used for determining the antimicrobial activity of the prepared compounds against the selected pathogenic microorganisms. DFT studies are performed using Gaussian 09 software 6-31G/B3LYP set.

Synthesis of Schiff base (L_1): The isoniazid-based Schiff base was synthesized by reacting isoniazid and salicylaldehyde in a 1:1 molar ratio (10 mmol each) in 30 mL of ethanol. The reaction mixture was then treated under reflux for 3 h at 60-80 ºC. After completion, a colourless precipitate formed, which was subsequently filtered and dried under vacuum (**Scheme-I**).

Synthesis of mixed ligand Schiff base metal(II) complexes: The isoniazid-based Schiff base (L_1), synthesized in a 1:1 molar ratio, was thoroughly mixed with the corresponding metal chloride salt (MCl_2) [Co(II), Ni(II), Cu(II), Zn(II)] in ethanolic solution for 30 min. Subsequently, a 1 mM ethanolic solution of lawsone (L_2) was added to the reaction mixture. The entire blend was stirred for 4 h, after which the reaction mixture was filtered, dried and recrystallized from hot ethanol (**Scheme-I**). The resulting metal complexes followed the $[ML_1L_2(H_2O_2)]$ (1:1:1) stoichiometry.

DNA binding studies: The DNA-binding interactions of the synthesized metal(II) complexes were evaluated using calf thymus DNA (*ct*-DNA) in a Tris-HCl buffer (5 mM Tris-HCl/50 mM NaCl, pH 7.2). The *ct*-DNA concentration was varied from 0 to 10 mM, while maintaining an invariable quantity of the metal(II) complexes (3 mL). The binding constant (K_b) was determined using the Wolf-Shimmer equation, by a plot of $[DNA]/(\varepsilon_a - \varepsilon_f)$ *vs.* [DNA]. The solutions were subjected to equilibrate at 25 ºC for 5 min after each addition of *ct*-DNA to the metal(II) complexes.

Viscosity measurements were conducted *via* Ostwald's micro-viscometer, submerged in a thermostatically controlled water bath at a stable temperature of 30 ± 1 ºC. The fluidity of the solutions was recorded at different concentrations of the prepared complexes (10-60 mM) using a stopwatch, while keeping the DNA concentration constant at 50 mM. The results were analyzed by plotting $(\eta/\eta_o)^{1/3}$ *vs.* [complex]/[DNA], where η represents the intrinsic viscosity of DNA and η_o refers to the viscosity of DNA in the presence of the synthesized complexes [31].

DFT studies: The Gaussian 09W software package was utilized to optimize the geometries of the synthesized compounds in the gas phase using the B3LYP/6-31+G(d,p) basis

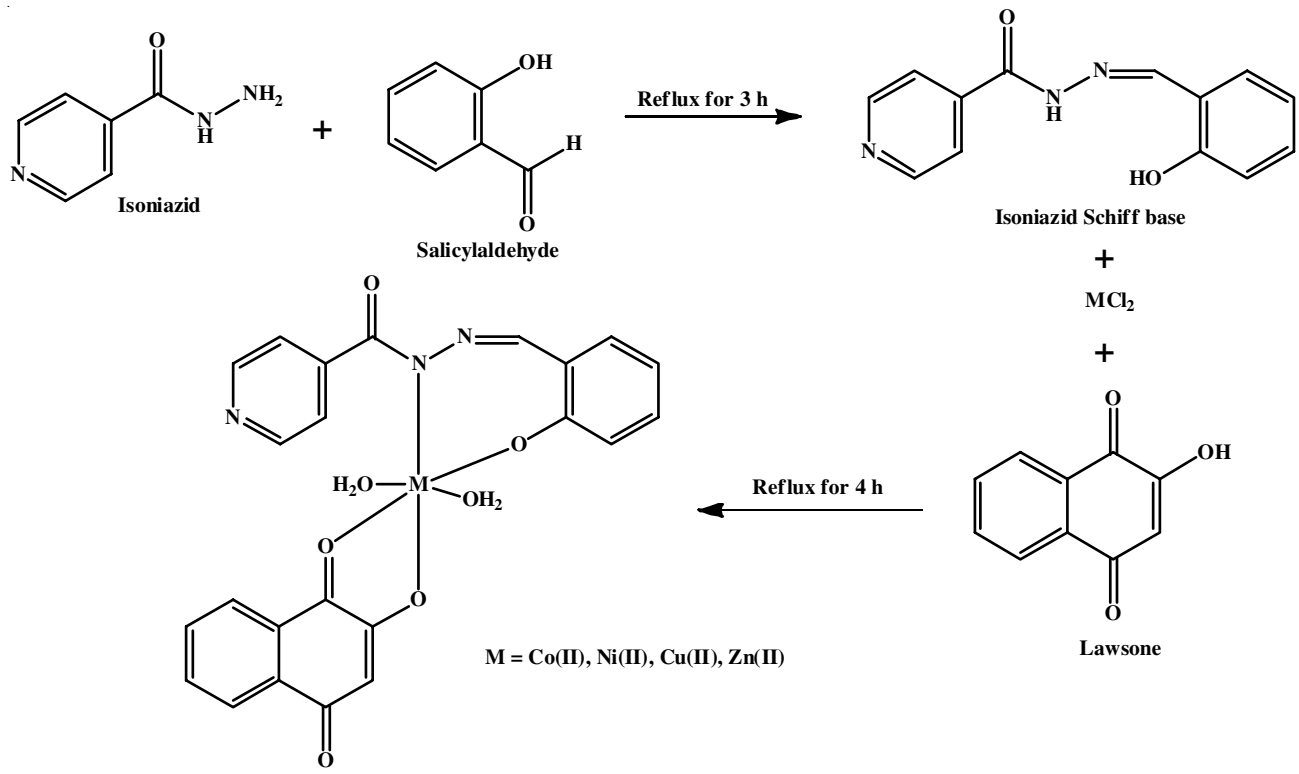

Scheme-I: Synthetic route of Schiff base ligand and its mixed ligand transition metal(II) complexes

set for both the ligand and its metal(II) complexes. The input data were visualized and the HOMO-LUMO energy values were extracted using the Gaussian View molecular visualization program. Furthermore, various chemical reactivity parameters were determined using Koopmans' theorem, including chemical potential (μ), global hardness (η), chemical softness (S) and electrophilicity (ω) [32,33].

Antimicrobial assay: The effect of the synthesized metal(II) complexes against the microbes was assessed using the broth dilution method against Gram-positive bacteria (*S. aureus*, *B. subtilis*) and Gram-negative bacteria (*E. coli*, *S. typhi*, *P. vulgaris*). The antifungal activity was also tested against *A. niger*, *C. albicans*, *C. lunata*, *A. flavus* and *R. bataticola*. The minimum inhibitory concentration (MIC) values of the synthesized compounds were compared with those of standard drugs, including ciprofloxacin (for antibacterial activity) and fluconazole (for antifungal activity) [34,35].

RESULTS AND DISCUSSION

The synthesized Schiff base and its metal(II) complexes exhibited high stability at room temperature. It was observed that Schiff base has greater solubility in ethanol and methanol, whereas the metal(II) complexes were soluble only in DMSO and DMF. The non-appearance of chloride counterions in the complexes was confirmed using Volhard's test. The physico-chemical parameters of the synthesized Schiff base ligand and its metal(II) complexes are given in Table-1.

IR spectral studies: The FTIR spectrum of the Schiff base ligand displayed a characteristic imine (-CH=N) stretching vibration at 1654 cm^{-1}. A shift to lower frequencies (1550-1525 cm^{-1}) in the synthesized metal(II) complexes suggests a reduction in the C=N double bond character, indicating coordination with the metal center. The additional absorption bands observed in the 1643-1620 cm^{-1} range correspond to C=O stret-

TABLE-1
PHYSICO-CHEMICAL PARAMETERS OF THE SYNTHESIZED SCHIFF BASE AND THE METAL(II) COMPLEXES

Compound (m.f.)	Yield (%)	Colour	Elemental analysis (%): Calcd. (found)				m.w.	μ_{eff} (BM)	λ_m
			M	C	H	N			
L_1 ($C_{13}H_{11}N_3O_2$)	85	Colourless	–	64.72 (63.93)	4.60 (4.34)	17.42 (17.31)	241.25	–	–
Complex **1** ($CoC_{23}H_{18}N_3O_7$)	65	Brown	11.62 (11.55)	54.45 (54.42)	3.58 (3.48)	8.28 (8.18)	507	5.92	23
Complex **2** ($NiC_{23}H_{18}N_3O_7$)	73	Reddish brown	11.57 (11.52)	54.48 (54.39)	3.58 (3.49)	8.29 (8.25)	507	2.18	12
Complex **3** ($CuC_{23}H_{18}N_3O_7$)	79	Brownish yellow	12.41 (12.37)	53.96 (53.91)	3.54 (3.52)	8.21 (8.16)	512	1.86	19
Complex **4** ($ZnC_{23}H_{18}N_3O_7$)	59	Yellow	12.73 (12.69)	53.77 (53.74)	3.53 (3.52)	8.18 (8.10)	514	Diamagnetic	15

ching vibrations, attributed to the carbonyl group of isoniazid and lawsone (Fig. 1). A broad band at 3245 cm^{-1} in all the metal(II) complexes confirms the presence of coordinated water molecules. Furthermore, absorption bands in the 550-537 cm^{-1} range indicate the M–O bond formation, while bands appearing at 438-427 cm^{-1} correspond to M–N bonding in the complexes [36,37]. A comparison of FTIR vibrational frequencies between the free ligand and its metal complexes provided valuable insights into the coordination sites involved in metal binding. Changes in the characteristic peaks of key functional groups indicated potential coordination interactions.

Electronic spectra and magnetic properties of metal(II) chelates: The geometry of all the metal(II) complexes was predicted using UV-Vis spectroscopy, which serves a vital part in understanding the electronic transitions within a compound. In this study, the electronic spectra of the complexes were recorded in DMSO solvent and the results indicate an octahedral geometry for the metal(II) complexes.

The UV-Vis spectrum of the Schiff base ligand exhibited an absorption band at 34,481 cm^{-1}, corresponding to the π–π transition of the -C=N group. Another absorption band at 28,541 cm^{-1} was attributed to the n–π transition from the azomethine group [38]. For copper(II) complex, an absorption peak at 14,641 cm^{-1} was assigned to the *d–d* transition ($^2E_g \rightarrow {}^2T_{2g}$) (Fig. 2), confirming its octahedral geometry. The experimental magnetic susceptibility value of the Cu(II) complex was found to be 1.86 BM, further supporting its O_h geometry.

In nickel(II) complex, a characteristic band at 15,037 cm^{-1} corresponds to the $^3A_{2g}(F) \rightarrow {}^3T_{1g}(F)$ transition, confirming its octahedral structure. Similarly, the cobalt(II) complex displayed absorption bands at 16,450 cm^{-1} and 17,683 cm^{-1}, attributed to the $^4T_{1g}(F) \rightarrow {}^4T_{2g}(F)$ and $^4T_{1g}(F) \rightarrow {}^4T_{1g}(P)$ transitions, respectively, which align with an octahedral geometry for Co(II). The zinc(II) complex exhibited an absorption band at 24,551 cm^{-1}, corresponding to ligand-to-metal charge transfer (LMCT) rather than a *d–d* transition, due to its fully filled d^{10} configuration. The octahedral geometry of the Zn(II) complex was further confirmed through elemental analysis and additional characterization techniques [39].

Mass spectral studies: The molecular ion peaks observed in the ESI-mass spectra of both the Schiff base and the cobalt(II) complex align with their proposed molecular formulae (Fig.

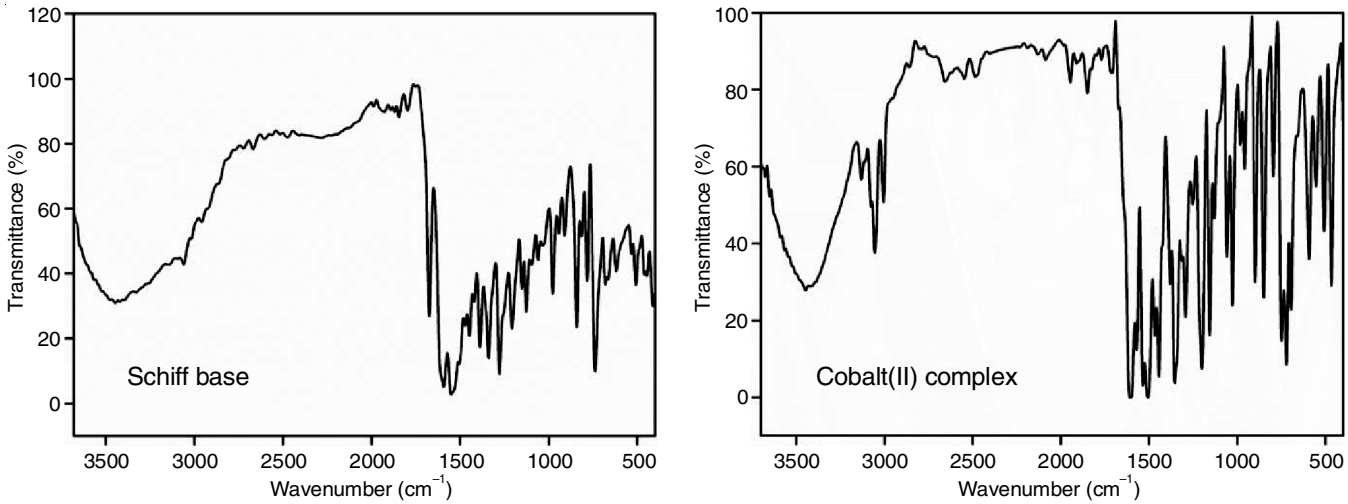

Fig. 1. IR spectra of Schiff base ligand and its cobalt(II) complex

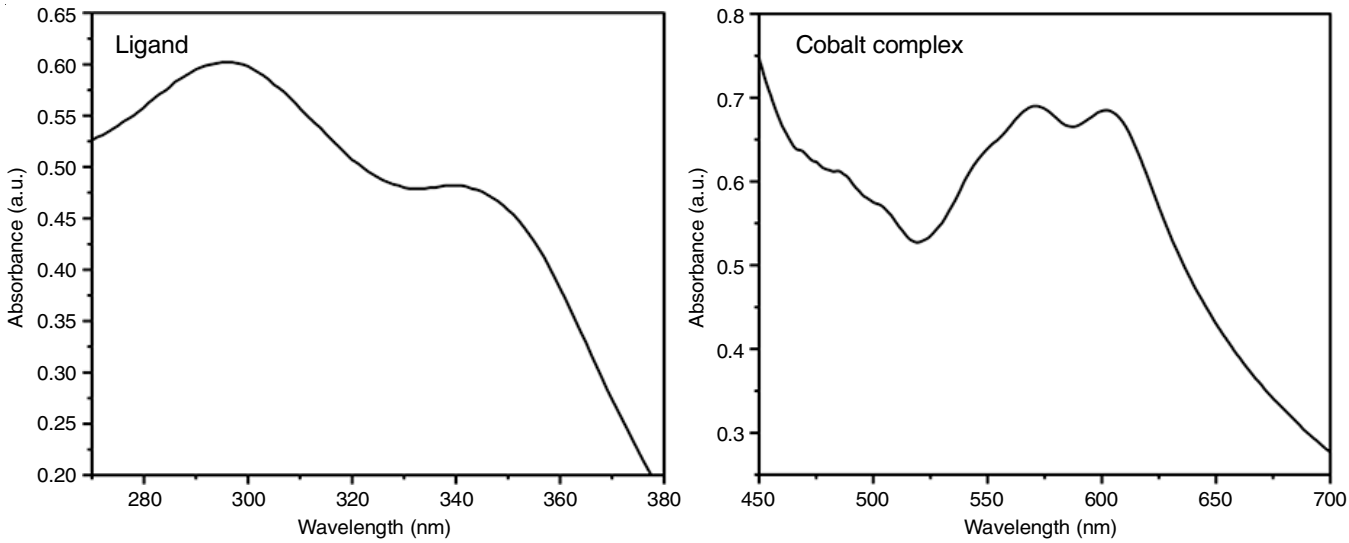

Fig. 2. UV spectra of Schiff base ligand and its copper(II) complex

3). The Schiff base exhibits a molecular ion peak at *m/z* 241, corresponding to the $[C_{13}H_1N_3O]^{+\bullet}$ species. Furthermore, the fragment peaks were detected at *m/z* 227, 211, 137 and 120, which correspond to $[C_{13}H_{10}N_3O]^+$, $[C_{13}H_{13}N_3]^+$, $[C_6H_7N_3O]^+$ and $[C_7H_8N_2]^+$, respectively.

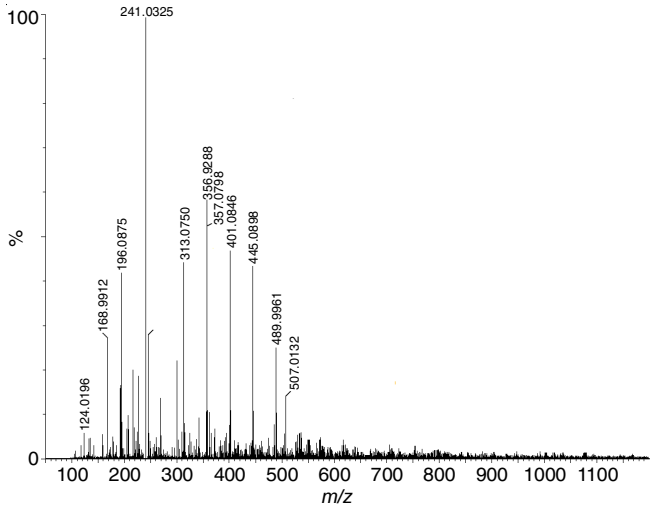

Fig. 3. Mass spectrum of complex **1**

For complex **3**, a molecular ion peak appears at *m/z* 512, which matches the molecular weight of the complex with the formula $C_{23}H_{18}N_3O_7Cu$. The stoichiometry of the complex is further established by the *m/z* values of the Schiff base and its corresponding components. The detected peaks and their molecular formulae aligned well with results obtained from other analytical techniques, reinforcing the structural validity of the proposed complex.

^{1}H NMR spectra: The ^{1}H NMR spectra of the Schiff base and the diamagnetic complex **4** were recorded in DMSO-d_6 using TMS as an internal standard. In the ^{1}H NMR analysis of both the ligand and complex **4**, multiplet peaks appearing in the 7.64-7.87 ppm range confirm the presence of an aromatic group. The singlet peak at 7.37 ppm in the ligand experiences a slight downfield shift to 8.23 ppm upon complexation. This shift suggests a deshielding effect indicating that the azomethine proton participates in coordination with the metal ion [40].

^{13}C NMR spectra: The ^{13}C NMR spectra of the Schiff base and its complex **4** exhibit peaks in the 109-135 ppm range, confirming the presence of aromatic carbon. The imine carbon (C=N) signals for the ligand and the zinc complex appear at 154.99 ppm and 153.89 ppm, respectively. These shifts in the frequency indicate the chelation of the azomethine (C=N) group to the metal ion [41].

Molar conductance: The conductivity values of all metal(II) complexes were measured in DMSO at room temperature. The observed conductance values ranged between 12 and 23 Ω^{-1} cm^2 mol^{-1}. According to Geary's classification, these values confirmed the non-electrolytic nature of the complexes [42].

In vitro analysis

DNA binding examination: DNA binding analysis is essential for understanding the interaction between compounds and nucleic acids. A decrease in absorbance with increasing *ct*-DNA concentration indicates an intercalative binding mode, which encompasses strong π-stacking interactions between DNA base pairs and an aromatic chromophore.

To investigate this, the electronic absorption spectra of the metal(II) complexes **1-4** were recorded individually after adding DNA at varying concentrations (30-150 μM). The observed hypochromism ranged from 6.53% to 10.92%, accompanied by a red shift of 1-5 nm (Table-2) [43]. These spectral changes confirmed the intercalative binding mechanism, attributed to π-stacking of phenyl rings between DNA base pairs (Fig. 4). The binding constants (K_b) for the complexes were determined and given as follows: Complex **1**: 6.48×10^4 M^{-1}, complex **2**: 7.95×10^4 M^{-1}, complex **3**: 8.89×10^4 M^{-1}, complex **4**: 7.12×10^4 M^{-1}. These values indicate an intercalation of the metal(II) complexes with the DNA [44-46]. Complex **3** exhibits the highest binding affinity.

TABLE-2
UV-SPECTRAL PARAMETERS OF THE COMPLEXES WITH THE ADDITION OF *ct*-DNA

Compound	λ_{max}		Δλ	H (%)	$K_b \times 10^4$ (M^{-1})
	Free	Bound			
Complex **1**	398	402	4	8.74	6.48
Complex **2**	325	329	4	6.53	7.95
Complex **3**	325	328	3	10.92	8.89
Complex **4**	322	321	1	9.03	7.12

Cyclic voltammetric: The cyclic voltammetric experiments for the metal(II) complexes were performed in DMSO, both in the absence and presence of *ct*-DNA. A positive shift in electrode potential upon DNA addition indicates an intercalative binding mode. The cyclic voltammograms of the metal(II) complexes, recorded before and after *ct*-DNA addition, is presented in Fig. 5. During the one-electron transfer redox process, the I_{pa}/I_{pc} ratio was found to be less than 1, confirming that the reaction occurring at the glassy carbon electrode surface is quasi-reversible [47,48]. A summary of all electrochemical parameters is provided in Table-3.

TABLE-3
ELECTROCHEMICAL PARAMETERS FOR THE *ct*-DNA BINDING INTERACTIONS OF THE METAL(II) COMPLEXES

Compound	$E_{1/2}$ (V)		ΔE_p (V)		ip_a/ip_c
	Free	Bound	Free	Bound	
Cobalt(II) complex	0.531	0.546	-0.243	-0.252	0.93
Nickel(II) complex	0.524	0.532	0.223	0.211	0.79
Copper(II) complex	0.621	0.633	-0.487	-0.482	0.88
Zinc(II) complex	0.312	0.334	0.413	0.436	0.92

Viscosity examination: The basis for studying DNA binding through viscosity observations is the change in DNA length that occurs when a molecule interacts with it. By monitoring changes in viscosity as the complexes' concentration rises, the DNA interaction mechanism of complexes **1-4** has been investigated. The intercalative binding is confirmed by the rising viscosity following the addition of the chemicals. Fig. 6 shows the viscosity of DNA plotted against [complex]/[DNA] *vs.* $(\eta/\eta_o)^{1/3}$. The expansion of the DNA helix is the reason for the observed increase in viscosity. The relative viscosity of

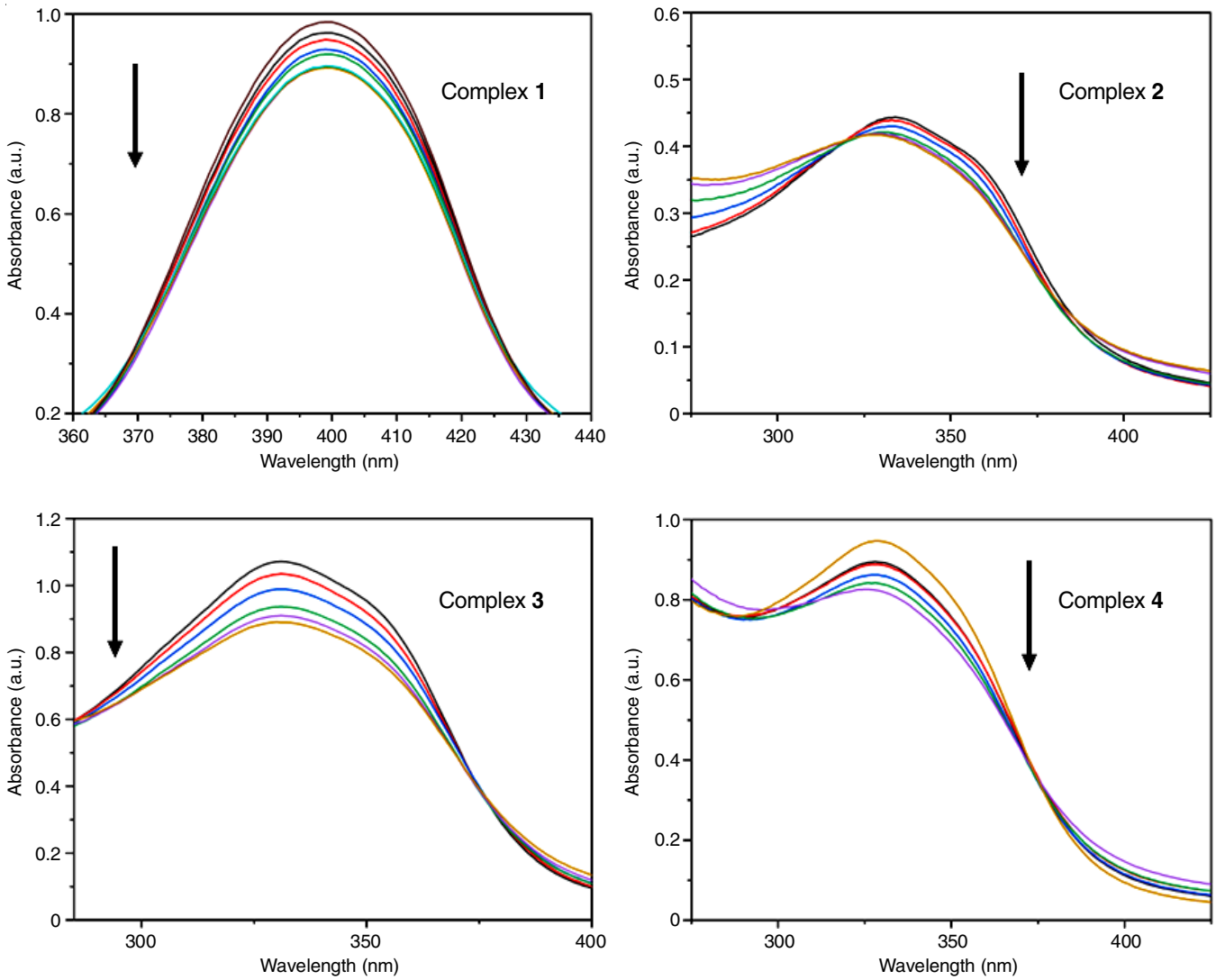

Fig. 4. DNA binding studies using absorption studies. The arrow is an indicator of the decreased absorbance with increased concentration

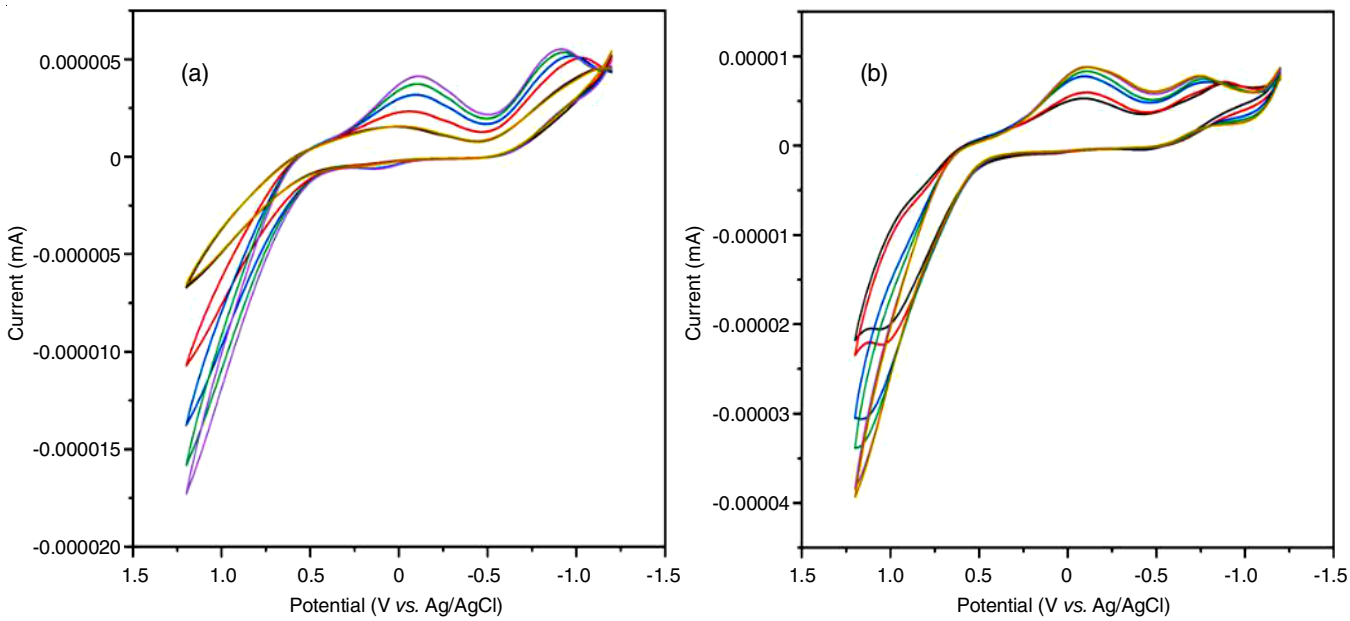

Fig. 5. Cyclic voltammograms of complex **3** (a) and complex **4** (b) in the presence of varying amount of *ct*-DNA

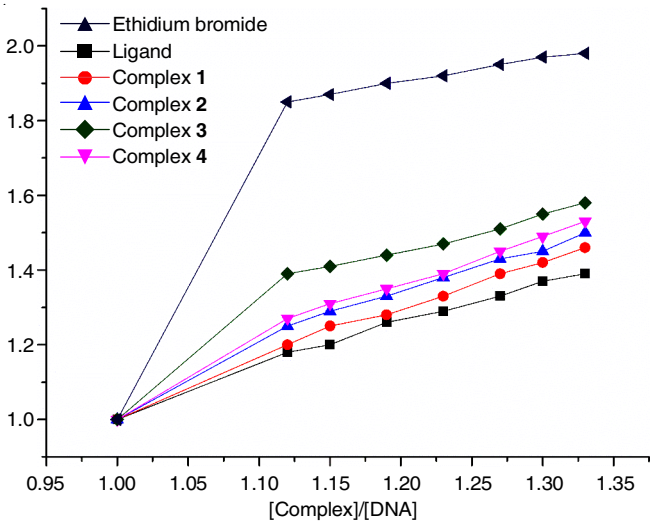

Fig. 6. Consequences of incremental amount of EB and the metal(II) complexes, on the relative viscosity of *ct*-DNA

ct-DNA rises as follows: Ethidium bromide > complex **3** > complex **4** > complex **2** > complex **1** > Ligand. The results of the absorption investigations and the viscosity examination closely matched.

Antimicrobial activity: The activity of the metal(II) complexes and the Schiff base against microbes like bacteria and fungi were evaluated *in vitro*. In addition to Gram-positive bacteria (*B. subtilis* and *S. aureus*) and Gram-negative bacteria (*S. typhi*, *P. vulgaris* and *E. coli*), the compounds were evaluated against the fungi (*A. niger*, *A. flavus*, *R. bataticola*, *C. lunata* and *C. albicans*). Ciprofloxacin and fluconazole were selected as the benchmark substances for evaluating the activity against microbes like bacteria and fungi. The metal(II) complexes exhibit stronger activity than the Schiff base ligand due to their lower minimum inhibition concentration, as indicated by the measured minimum inhibitory constant values (Table-4). This concept can be elucidated by Tweedy's chelation theory and Overton's hypothesis, which suggests that due to their non-polar nature, metal complexes can penetrate and disrupt lipophilic bacterial membranes [49-52].

In silico studies

ADMET properties: A free online program called SWISS ADME can be used to forecast a range of physico-chemical parameters, including the number of HBD and HBA, rotatable bonds, TPSA, log P and more. The data on the several factors obtained from the SWISS-ADME program is shown in Table-5. According to the findings, the compounds follow Lipinski's rule of five, with the exception of metal complexes, which deviate from it in terms of molecular weight. The number of hydrogen bond donors are within five and the number of hydrogen bond acceptors are within ten. Moreover, their strong bioavailability score, which is greater than 0.5, is complemented by log P values that are less than 5 and good total polar surface and solubility values. Because of their polarity, all the metal(II) complexes have good gastrointestinal absorption. The ligand's synthetic accessibility rating of 2.26 indicates that it can be synthesized easily, while the synthetic accessibility values of the complexes fall in the middle of the ranking range of 0-10 [53,54].

DFT studies: Using the B3LYP basis set, the DFT analyses were carried out in Gaussian 09W software. For the ligand and the metal(II) complexes (**1-4**) the shape optimization of the synthesized, Frontier molecular orbitals and reactivity characteristics were theoretically examined. Frontier orbitals or HOMO

TABLE-4
ANTIMICROBIAL ACTIVITY DATA OF SCHIFF BASE AND THE METAL(II) COMPLEXES

Compound	Minimum inhibitory concentration (MIC) (μM)									
	Antibacterial activity					Antifungal activity				
	B. subtilis	*S. aureus*	*E. coli*	*S. typhi*	*P. vulgaris*	*A. niger*	*A. flavus*	*C. albicans*	*R. bataticola*	*C. lunata*
Ligand	16.9	18.7	19.4	18.6	24.9	12.3	12.8	14.6	17.9	12.6
Complex **1**	15.6	17.2	17.6	16.2	16.7	11.0	13.2	14.3	11.6	10.7
Complex **2**	15.8	14.4	17.8	16.8	15.9	11.2	12.5	13.5	11.3	11.6
Complex **3**	12.7	13.5	13.8	14.6	15.2	9.7	12.6	12.5	10.3	10.1
Complex **4**	16.3	18.6	18.2	15.5	20.4	12.0	13.2	14.2	12.8	12.5
Ciprofloxacin	2.3	1.8	1.5	2.8	3.0	–	–	–	–	–
Fluconazole	–	–	–	–	–	1.4	1.6	1.9	1.5	1.6

TABLE-5
SWISS-ADME RESULTS OF SCHIFF BASE AND THE METAL(II) COMPLEXES

Parameters	Ligand	Cobalt complex	Nickel complex	Copper complex	Zinc complex
Molecular weight (g/mol)	241.25	507.08	507.08	512.07	514.07
No. of HBA	4	8	8	8	8
No. of HBD	2	2	2	2	2
No. of RB	4	2	2	2	2
TPSA (Å)^2	74.58	91.71	91.71	91.71	91.71
MLog P	0.79	-0.99	-0.99	-0.99	-0.99
Gastrointestinal absorption	High	High	High	High	High
Bioavailability score	0.55	0.56	0.56	0.56	0.56
Synthetic accessibility	2.26	5.33	5.20	5.26	5.41

HBA = Hydrogen bond acceptor, HBD = Hydrogen bond donor, RB = Rotatable bonds, TPSA = Topological polar surface area

and LUMO images of the metal(II) complexes are displayed in Fig. 7. The computed reactivity parameters of the compounds are shown in Table-6 [55].

While the LUMO is concentrated in the areas surrounding the coordination sites of the cobalt(II), copper(II), nickel(II) and zinc(II) complexes, the HOMO is concentrated over the

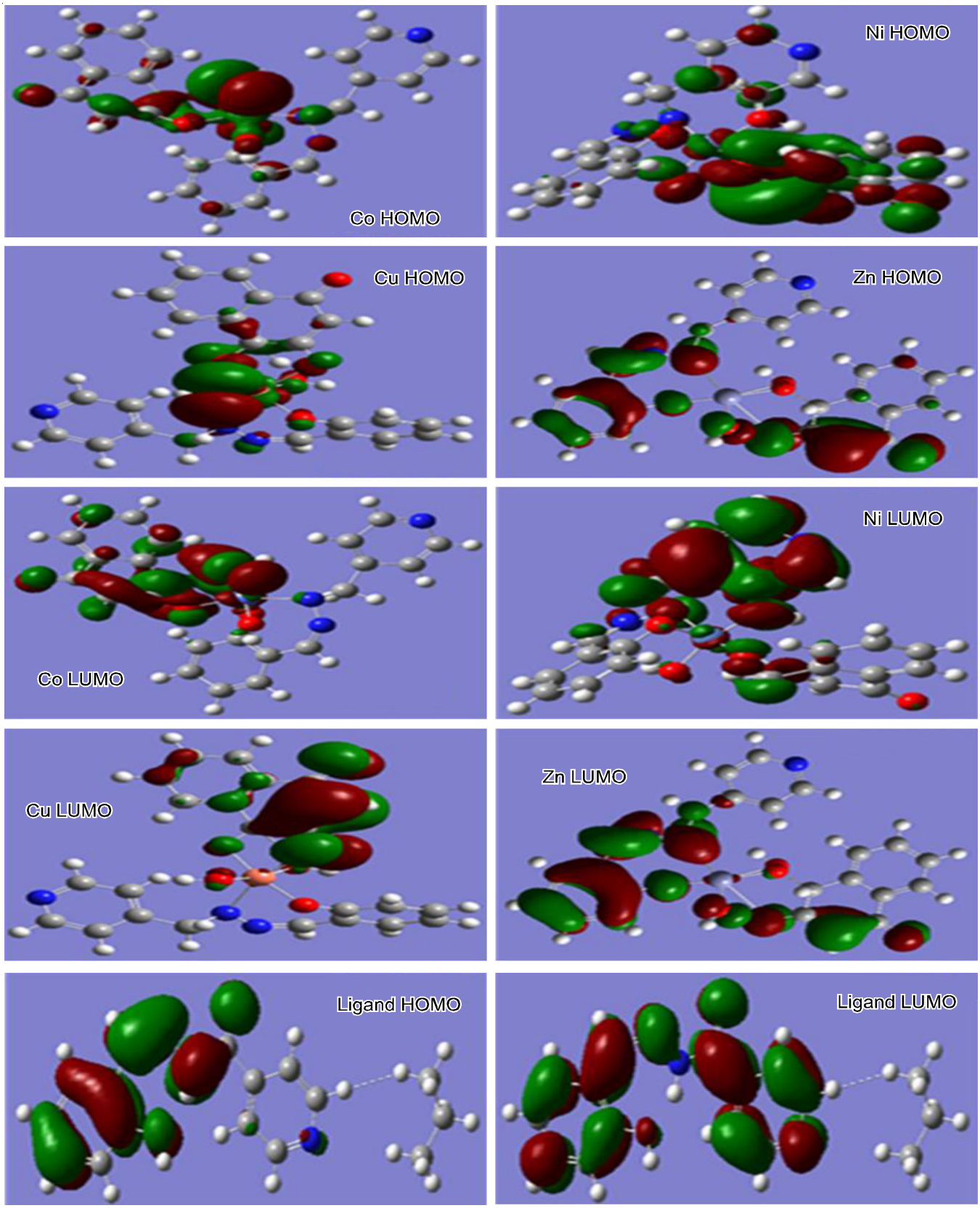

Fig. 7. HOMO-LUMO diagrams of the ligand and its metal(II) complexes

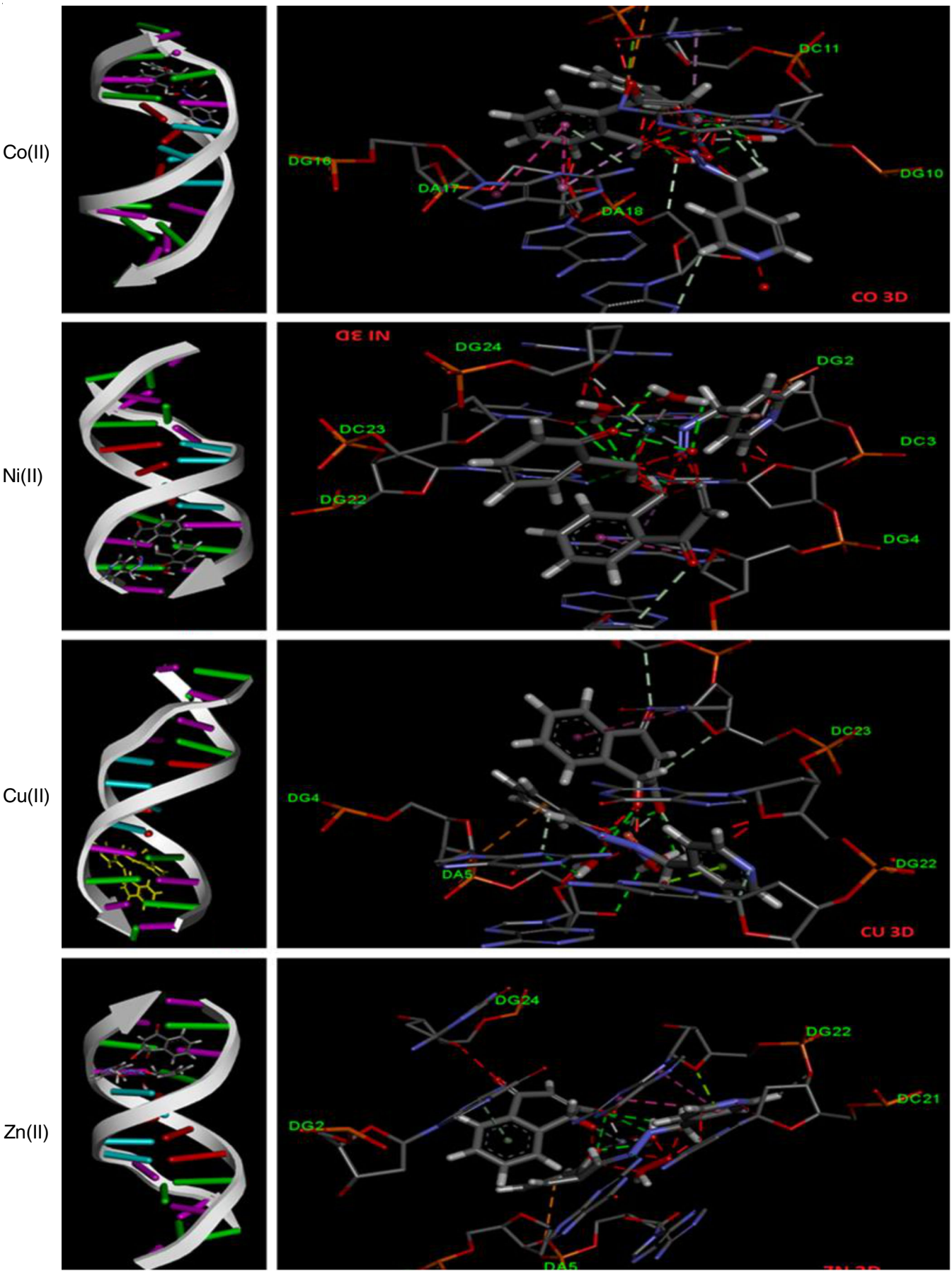

Fig. 8. 2D and 3D binding images of the compounds with DNA (PDB ID: 1BNA) receptor

TABLE-6
REACTIVITY PARAMETERS OF THE SCHIFF BASE AND COMPLEXES (**1-4**) IN GAUSSIAN SOFTWARE-09W

Parameters	Ligand	Co	Ni	Cu	Zn
Electronic energy (a.u)	-675.56	-5437.92	-5689.04	-5983.26	-5659.04
Dipole moment (Debye)	3.2	6.4	6.2	9.7	9.1
HOMO	-0.1545	-0.1616	-0.1653	-0.1895	-0.1602
LUMO	0.1211	0.1443	0.1407	0.0667	0.1195
ΔE (eV)	0.2757	0.3060	0.3061	0.2563	0.2797
Electronegativity (χ) (eV)	-0.0166	-0.0086	-0.0129	-0.0614	-0.0203
Global hardness (η)	0.1378	0.1530	0.1510	0.1281	0.1398
Chemical softness (S)	0.0687	0.0565	0.0585	0.0840	0.0699
Electrophilicity (ω)	0.0040	0.0009	0.00054	0.0147	0.0014

azomethine group, the other heteroatoms of the ligand and its metal complexes **1-4**. The compounds' stability is indicated by their negative HOMO and LUMO values. The fact that the complexes **1-4** have greater ΔE (eV) values than the ligand, which suggests that they are tougher and more stable. The ligand's softness indicates its stability and increased reactivity with the complexes' coordination site. Out of all the compounds, copper(II) complex has the highest dipole moment value, which indicates that it has the strongest biological contact and is efficient at crossing biological membranes [56].

Molecular docking studies: In this study, docking investigation was performed using the 1BNA receptor, obtained from the RCSB Protein Data Bank. The docking analysis was conducted with Hex 8.0 software and visualized using Discovery Studio Visualizer 4.0. Both the Schiff base ligand and the complexes **1-4** interact with the receptor primarily through hydrogen bonding. The compounds exhibit an intercalative binding mode, as they stack between the DNA base pairs. The binding energies for the docked compounds were recorded as follows: -233.54 kJ mol^{-1} (L_1), -344.32 kJ mol^{-1} (complex **1**), -308.86 kJ mol^{-1} (complex **2**), -332.31 kJ mol^{-1} (complex **3**) and -268.72 kJ mol^{-1} (complex **4**). The 2D and 3D interactions of these compounds with the 1BNA receptor are illustrated in Fig. 8. Based on the binding constant values, the copper(II) complex demonstrated significant interaction with DNA, which aligns well with the findings from *in vitro* absorption studies [57,58].

Conclusion

In this study, four novel mixed-ligand transition metal(II) Schiff base complexes were synthesized through the condensation of isoniazid and salicylaldehyde (as primary ligand) with lawsone as the co-ligand. The synthesized complexes were characterized using various analytical and spectroscopic techniques, confirming their octahedral geometry. The optimized molecular structure and theoretical reactivity parameters were determined using Gaussian 09 W software. The pharmacokinetic and biological features of the compounds were assessed using SWISS-ADME software. The antimicrobial evaluations demonstrated that these complexes exhibit strong inhibitory activity against multiple bacterial and fungal strains. The intercalative binding potential of the designed compounds was explored with electronic absorption titrations and viscosity measurements, further validated by molecular docking studies. A comparison between the DFT-based theoretical predictions and experimental findings showed the excellent agreement.

ACKNOWLEDGEMENTS

The authors express their heartfelt thankfulness to the VHNSN College Managing Board, Principal and Head of the Department of Chemistry for supporting the research with all the adequate facilities.

CONFLICT OF INTEREST

The authors declare that there is no conflict of interests regarding the publication of this article.

REFERENCES

1. E. Raczuk, B. Dmochowska, J. Samaszko-Fiertek and J. Madaj, *Molecules*, **27**, 787 (2022); https://doi.org/10.3390/molecules27030787
2. A.K. Jangid, R. Solanki, S. Patel, K. Medicherla, D. Pooja and H. Kulhari, *ACS Omega*, **7**, 15919 (2022); https://doi.org/10.1021/acsomega.2c01041
3. J. Ceramella, D. Iacopetta, A. Catalano, F. Cirillo, R. Lappano and M.S. Sinicropi, *Antibiotics*, **11**, 191 (2022); https://doi.org/10.3390/antibiotics11020191
4. N. Kumar, R. Kaushal and P. Awasthi, *J. Mol. Struct.*, **1288**, 135751 (2023); https://doi.org/10.1016/j.molstruc.2023.135751
5. M.N. Uddin, S.S. Ahmed and S.M.R. Alam, *J. Coord. Chem.*, **73**, 3109 (2020); https://doi.org/10.1080/00958972.2020.1854745
6. N.K. Chaudhary, B. Guragain, S.K. Chaudhary and P. Mishra, *Bibechana*, **18**, 214 (2021); https://doi.org/10.3126/bibechana.v18i1.29841
7. M.S. Hossain, P.K. Roy, R. Ali, C.M. Zakaria and M. Kudrat-E-Zahan, *Clin. Med. Res.*, **6**, 177 (2017); https://doi.org/10.11648/j.cmr.20170606.13
8. S. Abdolmaleki, A. Aliabadi and S. Khaksar, *Coord. Chem. Rev.*, **531**, 216477 (2025); https://doi.org/10.1016/j.ccr.2025.216477
9. P. Kumar and M. Nath, *J. Mol. Struct.*, **1300**, 137250 (2024); https://doi.org/10.1016/j.molstruc.2023.137250
10. A.A. Mohamed, F. Ahmed, W.A. Zordok, W.H. El-Shwiniy, S.A. Sadeek and H.S. Elshafie, *Inorganics*, **10**, 177 (2022); https://doi.org/10.3390/inorganics10110177
11. M. Štiblariková, A. Lásiková and T. Gracza, *Mar. Drugs*, **21**, 19 (2022); https://doi.org/10.3390/md21010019
12. N. Kerru, L. Gummidi, S. Maddila, K.K. Gangu and S.B. Jonnalagadda, *Molecules*, **25**, 1909 (2020); https://doi.org/10.3390/molecules25081909
13. A. Palanimurugan, A. Dhanalakshmi, P. Selvapandian and A. Kulandaisamy, *Heliyon*, **5**, e02039 (2019); https://doi.org/10.1016/j.heliyon.2019.e02039
14. V. Judge, B. Narasimhan and M. Ahuja, *Med. Chem. Res.*, **21**, 3940 (2012); https://doi.org/10.1007/s00044-011-9948-y

15. F.A.R. Rodrigues, I.S. Bomfim, B.C. Cavalcanti, C.Ó. Pessoa, J.L. Wardell, S.M.S.V. Wardell, A.C. Pinheiro, C.R. Kaiser, T.C.M. Nogueira, J.N. Low, L.R. Gomes and M.V.N. de Souza, *Bioorg. Med. Chem. Lett.*, **24**, 934 (2014); https://doi.org/10.1016/j.bmcl.2013.12.074
16. M. Kabak, A. Elmali and Y. Elerman, *J. Mol. Struct.*, **477**, 151 (1999); https://doi.org/10.1016/S0022-2860(98)00604-8
17. A.C. González-Baró, R. Pis-Diez, B.S. Parajón-Costa and N.A. Rey, *J. Mol. Struct.*, **1007**, 95 (2012); https://doi.org/10.1016/j.molstruc.2011.10.026
18. V. Ferraresi-Curotto, G.A. Echeverría, O.E. Piro, R. Pis-Diez and A.C. González-Baró, *Spectrochim. Acta A Mol. Biomol. Spectrosc.*, **137**, 692 (2015); https://doi.org/10.1016/j.saa.2014.08.095
19. M. Kushiro, H. Hatabayashi, Y. Zheng and K. Yabe, *Mycoscience*, **58**, 85 (2017); https://doi.org/10.1016/j.myc.2016.10.002
20. M.E. Reichmann, S. Rice, C.A. Thomas and P. Doty, *J. Am. Chem. Soc.*, **76**, 3047 (1954); https://doi.org/10.1021/ja01640a067
21. J.B. Chaires, N. Dattagupta and D.M. Crothers, *Biochemistry*, **21**, 3933 (1982); https://doi.org/10.1021/bi00260a005
22. R. Bielski and G. Grynkiewicz, *Green Chem.*, **23**, 7458 (2021); https://doi.org/10.1039/D1GC02402G
23. D.R. Boer, A. Canalsa and M. Coll, *Dalton Trans.*, 399 (2009); https://doi.org/10.1039/B809873P
24. J. Sheng, J. Gan and Z. Huang, *Med. Res. Rev.*, **33**, 1119 (2013); https://doi.org/10.1002/med.21278
25. P. Kumar, S. Tomar, K. Kumar and S. Kumar, *Dalton Trans.*, **52**, 6961 (2023); https://doi.org/10.1039/D3DT00368J
26. E. Pahlavani, H. Kargar and N.S. Rad, *Zahedan J. Res. Med. Sci.*, **17**, e1010 (2015); https://doi.org/10.17795/zjrms1010.
27. M.T. Carter, M. Rodriguez and A.J. Bard, *J. Am. Chem. Soc.*, **111**, 8901 (1989); https://doi.org/10.1021/ja00206a020
28. T. Koopmans, *Physica*, **1**, 104 (1934); https://doi.org/10.1016/S0031-8914(34)90011-2
29. R.G. Parr and R.G. Pearson, *J. Am. Chem. Soc.*, **105**, 7512 (1983); https://doi.org/10.1021/ja00364a005
30. A. Mehta, A. Jain and G. Saxena, *Pharm. Biochem. Res.*, **8**, 301 (2022); https://doi.org/10.32598/PBR.8.4.1067.1
31. Y. Deswal, S. Asija, D. Kumar, D.K. Jindal, G. Chandan, V. Panwar, S. Saroya and N. Kumar, *Res. Chem. Intermed.*, **48**, 703 (2022); https://doi.org/10.1007/s11164-021-04621-5
32. O.M. Adly and H.F. El-Shafiy, *J. Coord. Chem.*, **72**, 218 (2019); https://doi.org/10.1080/00958972.2018.1564912
33. K. Nakamoto, Infrared and Raman Spectra of Inorganic and Coordination Compounds. Part A: Theory and Applications in Inorganic Chemistry; Part B: Application in Coordination, Organometallic, and Bioinorganic Chemistry, edn 5 Wiley: New York (1997).
34. R.A. Ammar, A.M. Alaghaz, M.E. Zayed and L.A. Albedair, *J. Mol. Struct.*, **1141**, 368 (2017); https://doi.org/10.1016/j.molstruc.2017.03.080
35. N. Raman, K. Pothiraj and T. Baskaran, *J. Mol. Struct.*, **1000**, 135 (2011); https://doi.org/10.1016/j.molstruc.2011.06.006
36. S.B. Jagtap, N.N. Patil, B.P. Kapadnis and B.A. Kulkarni, *Met. Based Drugs*, **8**, 159 (2001); https://doi.org/10.1155/MBD.2001.159
37. M. Selvaganapathy, N. Pravin, K. Pothiraj and N. Raman, *J. Photochem. Photobiol. B*, **138**, 256 (2014); https://doi.org/10.1016/j.jphotobiol.2014.06.003
38. R.M. Issa, A.M. Khedr and H.F. Rizk, *Spectrochim. Acta A Mol. Biomol. Spectrosc.*, **62**, 621 (2005); https://doi.org/10.1016/j.saa.2005.01.026
39. N. Gondia and S. Sharma, *J. Mol. Struct.*, **1171**, 619 (2018); https://doi.org/10.1016/j.molstruc.2018.06.010
40. M. Sönmez, M. Celebi and I. Berber, *Eur. J. Med. Chem.*, **45**, 1935 (2010); https://doi.org/10.1016/j.ejmech.2010.01.035
41. Q. Liang, P.D. Eason and E.C. Long, *J. Am. Chem. Soc.*, **117**, 9625 (1995); https://doi.org/10.1021/ja00143a002
42. W. Geary, *Coord. Chem. Rev.*, **7**, 81 (1971b); https://doi.org/10.1016/S0010-8545(00)80009-0
43. A.W. Wallace, W. Rorer Murphy Jr. and J.D. Petersen, *Inorg. Chim. Acta*, **166**, 47 (1989); https://doi.org/10.1016/S0020-1693(00)80785-9
44. G.M. Cohen and H. Eisenberg, *Biopolymers*, **8**, 45 (1969); https://doi.org/10.1002/bip.1969.360080105
45. Ü. Demirbas, B. Barut, A. Özel, F. Çelik, H. Kantekin and K. Sancak, *J. Mol. Struct.*, **1177**, 571 (2019); https://doi.org/10.1016/j.molstruc.2018.10.006
46. N. Shahabadi, S. Kashanian and F. Darabi, *Eur. J. Med. Chem.*, **45**, 4239 (2010); https://doi.org/10.1016/j.ejmech.2010.06.020
47. M. Dehkhodaei, M. Sahihi, H.A. Rudbari, S. Gharaghani, R. Azadbakht, S. Taheri and A.A. Kajani, *J. Mol. Liq.*, **248**, 24 (2017); https://doi.org/10.1016/j.molliq.2017.10.044
48. O.H. Al-Obaidi, *Open J. Inorg. Non-metallic Mater.*, **02**, 59 (2012); https://doi.org/10.4236/ojinm.2012.24007
49. T. Jeewoth, M.G. Bhowon and H.L.K. Wah, *Transition Met. Chem.*, **24**, 445 (1999); https://doi.org/10.1023/A:1006917704209
50. I.P. Ejidike and P.A. Ajibade, *Rev. Inorg. Chem.*, **35**, 191 (2015); https://doi.org/10.1515/revic-2015-0007
51. Z.H. Chohan, A. Munawar and C.T. Supuran, *Met. Based Drugs*, **8**, 137 (2001); https://doi.org/10.1155/MBD.2001.137
52. E. Halevas, A. Pekou, R. Papi, B. Mavroidi, A.G. Hatzidimitriou, G. Zahariou, G. Litsardakis, M. Sagnou, M. Pelecanou and A.A. Pantazaki, *J. Inorg. Biochem.*, **208**, 111083 (2020); https://doi.org/10.1016/j.jinorgbio.2020.111083
53. C.A. Lipinski, F. Lombardo, B.W. Dominy and P.J. Feeney, *Adv. Drug Deliv. Rev.*, **46**, 3 (2001); https://doi.org/10.1016/S0169-409X(00)00129-0
54. D.F. Veber, S.R. Johnson, H. Cheng, B.R. Smith, K.W. Ward and K.D. Kopple, *J. Med. Chem.*, **45**, 2615 (2002); https://doi.org/10.1021/jm020017n
55. M. Jafari, M. Salehi, M. Kubicki, A. Arab and A. Khaleghian, *Inorg. Chim. Acta*, **462**, 329 (2017); https://doi.org/10.1016/j.ica.2017.04.007
56. H.P. Ebrahimi, J.S. Hadi, Z.A. Abdulnabi and Z. Bolandnazar, *Spectrochim. Acta A Mol. Biomol. Spectrosc.*, **117**, 485 (2014); https://doi.org/10.1016/j.saa.2013.08.044
57. L. D'Anna, L. Marretta, A. Froux, S. Rubino, V. Butera, A. Spinello, R. Bonsignore, A. Terenzi and G. Barone, *Eur. J. Inorg. Chem.*, (2025); https://doi.org/10.1002/ejic.202400705
58. S. Maddikayala, K. Bengi, V. Malkhed and S.R. Pulimamidi, *Appl. Organomet. Chem.*, **39**, e7949 (2025); https://doi.org/10.1002/aoc.7949